Investigation of zeolite supported platinum electrocatalyst for electrochemical oxidation of small organic species

Jun Yao[1]* and Yufeng Yao[2]

[1] School of Engineering, University of Lincoln, Brayford Pool, Lincoln LN6 7TS, UK

[2] Department of Engineering Design and Mathematics, University of the West of England, Bristol BS16 1QY, UK

Highlights

- Pt ion exchange with Y type zeolite and calcination and reduction.
- H^+ spillover at electrode and solution interface and through zeolite framework.
- Pt particle size measurement by EXAFS.
- Pt electrocatalytic performance by CV measurement.
- Electro-oxidation of small organic species on Pt surface.

Abstract: Zeolite supported Pt electrocatalysts, made by ion exchange method using Pt/Y type zeolite, have been investigated to determine Pt electrochemical activity of HCOOH and CH_3OH oxidation using the cyclic voltammetry (CV) and the extended X-ray adsorption fine structure (EXAFS) techniques. The study reveals that the introduction of excess H^+ ions during electrocatalyst pre-treatment could enhance electrochemical reaction on Pt surface due to higher Pt dispersion, regardless of zeolite being a direct current electronic conducting insulator. Two possible conduction pathways might contribute to the electrocatalytic reaction on Pt surface with Pt particle size and loading: (1) hydrogen atoms/H^+ ions spillover through zeolite framework and at the electrode and solution interface; (2) surface mobility of adsorbed species on electrode surface. The water may act as a carrier in assisting the migration of the H^+ ions throughout zeolite channels to facilitate the charger and electron transfer in such an electrical system.

Keywords: Pt on Y zeolite, H^+ spillover species surface mobility, HCOOH and CH_3OH oxidation, CV, EXAFS.

1. Introduction

Carbon supported platinum (Pt/C) as a common type of electrocatalyst has been widely used in direct methanol fuel cell (DMFC) applications with Pt loading on carbon normally in a range of 20% - 40%, which is prohibitively expensive. Furthermore, the Pt/C electrocatalysts can contain large-size

*Correspondent author. Tel: +44 (0)1522 837 919
Email: jyao@lincoln.ac.uk

Pt particles that may decrease the electrocatalytic activity. Previous study by Min et al. [1] revealed the increase of specific activities with the decrease of the surface area for carbon supported Pt electrocatalyst, in which the oxygen reduction on Pt surface was a structure-sensitive reaction associated with the adsorption strength of oxygen intermediate on the Pt surface. Hence, considerable research efforts have been made in the past decades by developing a highly dispersed nanostructured Pt electrocatalyst to improve fuel cell efficiency and economic viability for energy applications.

Zeolite can provide an environment to produce highly dispersed Pt metal particle, owing to its high selectivity and great capacity of absorbing and retaining water by the creation of zeolite proton conducting membranes for solution like ionic conduction through interconnecting channels without damaging the zeolite crystalline lattice structure [2-4]. The growth of Pt particle on zeolite is mainly controlled by O_2 calcination step in gas phase and high dispersion of Pt can be achieved by further H_2 reduction step [5]. A slow heating process at a high O_2 flowrate would be preferable to avoid Pt non-uniform distribution on zeolite introduced by auto-reduction [6] that may produce large Pt metal particles during the removal of ammonia ligands at 300 ^oC [7-9]. Pt is also found favourable to remain in the zeolite supercage at 350 ^oC in O_2 and 400 ^oC in H_2, respectively, resulting in a particle size of 0.6 – 1.3 nm, which is much smaller than that of graphene based materials with Pt particle size growing up to 1.5 – 19 nm [10].

Pt was more stable at zeolite sodalite cage, mainly due to its strong polarization nature of the Pt-d bond electron configuration [11]. A high degree of Pt dispersion was reported in the presence of H^+ ions by forming Pt–H adduct in zeolite structure. H^+ ions can act as a chemical anchor to diminish the sintering of Pt particles at 400 ^oC in H_2. The polarization of Pt particles by the nearby cations, i.e. H^+, might result in the electron deficiency of Pt, leading to the change of Pt catalytic activity and spectroscopic properties [12, 13]. Moreover, the charge transfer between Pt and nearby neighbouring zeolite support oxygen atoms can play an important role during this process [14, 15].

The disorder of Pt particle on zeolite framework has had a dramatic effect on the Pt electronic structure by the extended X-ray adsorption fine structure (EXAFS) [16, 17]. The Pt-Pt bond distance was shortened to less than 2.75 *Å* than that of Pt bulk metal in the presence of strong charger transfer between Pt clusters with the increase of the Pt-Pt binding energy due to Pt electron deficiency [18], compared to Pt in a non-zeolite supported system, i.e. Pt/SiO_2. Vaarkamp et al. [19] predicted an average Pt particle size consisting of approximately 15 atoms with the first shell coordination number and Pt-Pt distance of 5.5 and 2.75 *Å*, respectively.

The electrochemical activity of Pt nanostructure on zeolite was previously investigated by Rolison et al. [4]. The Pt was found to exhibit particular chemical and physical characteristics that could enhance the electrochemical reaction, owing to high ionic strength between electrodes. Liu et al. [20] suggested that hydrogen spillover is an important process to promote Pt electrocatalysis for Pt/C electrode. The H^+ ions adsorbed on the Pt active surface could spillover and diffuse into the surface of the inert support to form acidic surface oxides for an interfacial reaction of electrocatalytic process being taken place on Pt surface. The spillover of hydrogen has been discovered in both Pt/Al_2O_3 and Pt/SiO_2 catalyst systems to promote the transport of an active species between catalyst active sites. Zhang et al. [21] also observed hydrogen spillover from Pt to zeolite Brønsted and Lewis acidic sites in gas phase.

Pt appears to be one of the best catalysts for dissociating the C-H bound at a relatively low potential [22], which is favourable to oxidise small organic species, such as, methanol (CH3OH) and formic acid (HCOOH). However, past studies showed that the high electrocatalytic activity of Pt for methanol oxidation can be attributed by both high dispersion of redox-active Pt nanocrystal and active sites in high surface area of catalyst support, i.e. ZSM-5 zeolite [23]. Hsieh et al. [24] also discovered that Pt catalyst supported by material containing oxygen function groups, e.g. graphene oxides, is much more favourable for HCOOH oxidation, owing to strong interactions between metal ions and oxidised substrates, thus limiting the CO poison on Pt surface. El-Nagar and Mohammed [25] has drawn a similar conclusion about an oxygen atmosphere being important to facilitate CO oxidation at a low potential level.

Zeolite can offer high active sites interconnected by oxygen atom to enhance Pt dispersion and nucleation. However, the electrochemical oxidation and the reduction of CH_3OH and HCOOH species on zeolite supported Pt with regard to hydrogen spillover process at the Pt/Y zeolite electrode and solution interface have not yet been fully investigated, since zeolite lacks the direct current (DC) electronic conduction, and the electro-organic reaction on Pt surface is generally a slow process due to the restriction of high current density generation [26].

In this study, laboratory made 1.5 wt% and 5 wt% loading Pt electrocatalysts with or without excess H^+ ions, introduced into zeolite structure by ion exchange method, will be investigated to determine the Pt electrochemical activity to oxidise CH_3OH and HCOOH species by cyclic voltammetry (CV). The Pt particle size and dispersion on zeolite will be characterised by EXAFS using a Nafion$^@$ bound electrode, fabricated by Pt/zeolite and carbon powder mixed with Nafion$^@$ to form ultra-thin film and membrane on electrode surface [2, 3]. The charger/electron transfer at electrode and solution interface will be investigated to understand Pt and zeolite conducting pathway, especially in the presence of excess H^+ ion on zeolite.

2. Experimental

2.1. Pt/Y zeolite electrocatalysts ion exchanged using $Pt(NH_3)_4(NO_3)_2$ or $Pt(NH_3)_4(NO_3)_2/NH_4NO_3$ salts

The 1.5 wt% and 5 wt% Pt loading on Y zeolite electrocatalysts was made by ion exchange method [17, 18] using $Pt(NH_3)_4(NO_3)_2$ salt (denoted as 15Ptancr4 for 1.5 wt% Pt loading and 5Ptancr4 for 5 wt% Pt loading on Y zeolite thereafter) or $Pt(NH_3)_4(NO_3)_2/NH_4NO_3$ salt (denoted as 15Ptanxcr4 for 1.5 wt% Pt loading and 5Ptanxcr4 for 5 wt% Pt loading on Y zeolite thereafter) in neutral solution, respectively.

An appropriate quantity of $Pt(NH_3)_4(NO_3)_2$ was thoroughly dissolved in 200 *ml* of triply distilled water. The ion exchange process was then taken place in water-jacketed reactor, where the sodium Y zeolite powder was dispersed at a concentration of 1 *g* per 100 *ml*. The Pt ion was slowly added by pumping $Pt(NH_3)_4(NO_3)_2$ salt solution into the reactor. The sample was then washed with triply distilled water until no $[Pt(NH_3)_4]^{2+}$ complex detected by Ultraviolet (UV) [27]. After washing, sample was later dried overnight in an oven.

In case of the excess nitrate ion exchange method using $Pt(NH_3)_4(NO_3)_2/NH_4NO_3$, the NH_4NO_3 was added firstly into the suspended zeolite using stoichiometric titration method to provide a NH_4NO_3 concentration of 0.063 *mol* dm^{-3} prior to the adding of the $Pt(NH_3)_4(NO_3)_2$ salt.

2.2. Calcination and Reduction

The synthesis of Pt nanostructures on Y zeolite was carried out by applying the calcination and reduction procedure to remove the Pt co-ordinate ligand, i.e. a crucial chemical step associated to the formation of Pt nano-particle dispersion on zeolite substrate [8].

$Pt(NH_3)_4(NO_3)_2$ salt Y zeolite samples were purged with argon at a moderate temperature in a fluidized bed reactor to dry out the water moisture. This will avoid the growth of large-size Pt particles [9]. After cooling, O_2 gas was introduced into the reactor to re-heat samples up to 350 ^oC. Then, samples were chemically reduced at a temperature of 400 ^oC by purging with 5% H_2 and 95% N_2 gas mixture to produce a fine Pt distribution on zeolite. The following equations present the Pt oxidation and reduction reactions [8]:

Oxidation $[Pt(NH_3)_4]^{2+} = NH_3\ (gas) + Pt^{2+}$ (1)

$O_2\ (gas) + 2Pt^{2+} = 2PtO$ (2)

Reduction: $PtO + H_2\ (gas) = H_2O + Pt$ (3)

For sample ion exchanged with NH_4NO_3 salt (prior to the adding of the $Pt(NH_3)_4(NO_3)_2$ salt), the sample was heated at 300 ^oC in argon to produce a fine distribution of the excess H^+ ions on zeolite framework using the reaction in equation (4) below. The Pt oxidation and reduction reactions after the introducing of $[Pt(NH_3)_4]^{2+}$ ions were followed by the same procedure presented in equations (1) – (3) .

$NH_4^+ = H^+ + NH_3\uparrow$ (4)

2.3. Electrochemical Cell and Cyclic Voltammetry

The electrode was made of electrocatalyst with 1.5 wt% and 5 wt% Pt loading on zeolite and (untreated) XC-72R carbon powder mixture mixed with 15 wt% Nafion$^@$ solution (i.e. 5 wt% solution in Aliphatic Alcohols and H_2O from Aldrich) as a binder. The resultant paste was then hot pressed on a sheet of 9 cm^2 carbon paper (E-TEK TGHP-90) for solidification. A disc of 2.5 cm^2 diameter of electrodes was then trimmed for CV measurement and a disc of 1.3 cm^2 for in-situ EXAFS measurement.

The charge separation on electrode was investigated in a glass-jacketed electrochemical cell, consisting of working electrode, Hg/Hg_2SO_4 Mercury/Mercuries Sulphate (MMS) reference electrode and a Pt gauze counter electrode. The in-situ EXAFS measurement was carried out in an electrochemical cell formed by two acrylic discs with two Kapton windows cut in the middle, accomplished by a working electrode connected with a gold wire current collector to reinforce the contact in the cell system via Pt gauze count electrode. The Hg/Hg_2SO_4 MMS reference electrode was then connected to the electrochemical cell using a salt bridge, re-assembled to produce a

sufficiently large absorption edge. The electrolyte was 2.5 *mol* dm^{-3} sulphuric acid (H_2SO_4) solution for the standard CV measurement and 1 *mol* dm^{-3} for the in-situ EXAFS measurement at a scan rate of 1 *mV* s^{-1} in a potential region of -0.65 *V* to 0.5 *V*, respectively, in which no solvent and electrolyte decomposition were detected [28].

For electro-oxidation reaction of HCOOH and CH_3OH species on Pt surface, the CV measurement was taken at 1 *mV* s^{-1} in an electrochemical cell containing 2.5 *mol* dm^{-3} sulphuric acid (H_2SO_4) and 1 *mol* dm^{-3} methanol or formic acid solution, until a clear and stable CV curve obtained.

2.4. The Extended X-ray Adsorption Fine Structure Measurement

EXAFS measurements were performed using a Synchrotron Radiation Source (SRS) at STFC Daresbury Laboratory, UK. The wiggler beam line was operated at conditions of 2 *GeV* and 100 *mA*. High-order harmonics that might affect the amplitude of EXAFS were removed using a double-crystal Si220 monochromator. The 50% detuning of harmonic beam using gas ion chambers filled with Ar, Xe or Kr and He was used to locate the Pt L_{III} absorption edge. A Pt foil was used as a reference sample for EXAFS data collection.

Data analysis was carried out using in-house software EXCURV 98. The inter-atomic distance, atom number and the type of backscattering neighbours were determined using a method proposed by Abruna [29].

3. Results and Discussion

3.1. Zeolite Brunauer-Emmett-Teller (BET) surface area measurement

Figure 1 depicts the zeolite BET surface area measurement to investigate zeolite structure change, owing to the calcination (O_2) and reduction (H_2) processes. The maximum 10% measurement uncertainty given by sample 15Ptancr4 (i.e. at 168 m^2g^{-1}) (see in table 1) is mainly due to the significant loss of zeolite crystal structure with merely 26.97% zeolite surface area preserved. The plain zeolite sample has shown the highest surface area measured at 623 m^2g^{-1}. By comparing to plain zeolite, it was found that about 86.52% of zeolite surface area was preserved by sample 15Ptanxcr4 (i.e. at 539 m^2g^{-1}), 90.37% and 88.76% by samples 5Ptanxcr4 (i.e. at 563 m^2g^{-1}) and 5Ptancr4 (i.e. at 553 m^2g^{-1}), respectively [30]. These data indicate that zeolite crystal structure is able to be well-preserved in the presence of excess H^+ ions (e.g. sample 15Ptanxcr4 or 5Ptanxcr4) during the calcination and reduction processes. The collapse of crystallized zeolite structure is found predominant for 1.5% Pt loading sample 15Ptancr4 without H^+ ion presence, possibly owing to the blockage of zeolite opening pores in small channels.

The surface area measured for XC-72R carbon powder is about 32.1% (i.e. at 200 m^2g^{-1}) compared to that of plain zeolite, slightly higher than the value given by sample 15Ptancr4. The carbon powder is only used as electrode binding paste in assisting to mix the Pt zeolite catalyst and Nafion@ polymer solution.

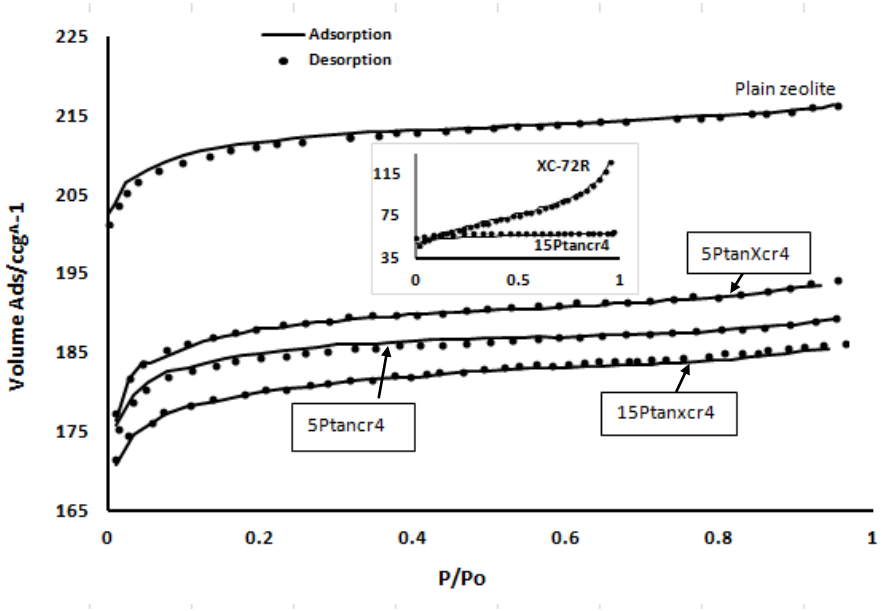

Fig. 1. Volumetric uptake of Nitrogen at a temperature of 77 Kelvin with adsorption in black solid lines and desorption in dotted symbols. All samples were made by calcination at 350 ^{o}C and reduction at 400 ^{o}C, respectively.

Table 1 BET Surface area measurement.

Sample	Plain zeolite	XC-72R	15Ptancr4	15Ptanxcr4	5Ptancr4	5Ptanxcr4
Surface area (m^2g^{-1})	623.2± 0.1%	200 ± 0.1%	168 ± 10%	539 ± 1.0%	553 ± 1.0%	563 ± 1.5%
Surface area preserved	100%	32.10%	26.97%	86.52%	88.76%	90.37%

3.2. Cyclic Voltammetry measurement in H_2SO_4 electrolyte solution

CV measurement was performed to determine the electro-activity of chemical species in the electrolyte solution on Pt surface by monitoring the current change against the potential. Figure 2 depicts a comparison of electrochemical activity between -0.65 *V* and 0.5 *V* for samples 15Ptancr4, 15Ptanxcr4, 5Ptancr4 or 5Ptanxcr4 Pt/Y zeolite | Nafion$^{@}$ bound working electrodes made by electrocatalyst with extra carbon powder mixture, respectively. The observed CV profile consists of very similar electrochemical behaviour with two distinguished hydrogen adsorption (HSP) and hydrogen reduction (HR) regions associated with the hydrogen adsorption peak (peak 'A'), hydrogen evaluation peak (peak 'B'), the re-oxidation peak (peak 'C') and desorption peak (peak 'D'), respectively.

A double layer (DL) current was measured at a potential range of -0.22 *V* to -0.40 *V* and -0.5 *V* to -0.33 *V*, during both cathodic and anodic sweeps. The current change in the hydride region provided by the electrode 15Ptanxcr4 has seen significantly larger in terms of magnitude, with a well-resolved

hydrogen oxidation peak captured at -0.64 *V*. The electrode 15Ptancr4 predicted a hydrogen adsorption peak being further shifted towards a positive potential direction at -0.58 *V*, compared to -0.62 *V* and -0.61 *V* determined by those of 5Ptancr4 and 5Ptanxcr4, respectively. This indicated that the energy level of hydrogen adsorption on Pt active sites for the electrode 15Ptanxcr4 was relatively high. No visible feature of hydrogen desorption peak 'D' was observed by the electrode 15Ptancr4, possibly due to very similar energy levels of these two sites, leading to insignificant oxidation and reduction redox surface group presence. The increase of hydrogen oxidation peak current was found to follow the order of samples as 15Ptanxcr4 -> 5Ptanxcr4 -> 5Ptancr4 -> 15Ptancr4. There was a weak hydrogen desorption peak captured in the anodic sweep by the electrodes 5Ptanxcr4 and 5Ptancr4, consistent to that shown by the electrode 15Ptanxcr4.

The presence of electron transfer at the electrode and solution interface was evidenced by the hydrogen adsorption, evolution and desorption peaks in hydride region. It was known that Pt electrocatalytic performance was closely associated with Pt particle sizes and their distributions on zeolite [14], due to the polarization of Pt particles by neighbouring cations, i.e. H^+, resulting in Pt electron deficiency. The significant hydrogen adsorption and evolution current change given by the electrode 15Ptanxcr4 has indicated the presence of high Pt distribution on zeolite.

Following equations describe an oxidation/reduction process on Pt surface:

$$Pt + H_2O = OHPt + H^+ + e^- \quad (5)$$

$$OHPt = PtO + H^+ + e^- \quad (6)$$

$$PtO + H^+ = Pt + OH^- \quad (7)$$

$$PtO + 2\,H^+ = Pt + H_2O \quad (8)$$

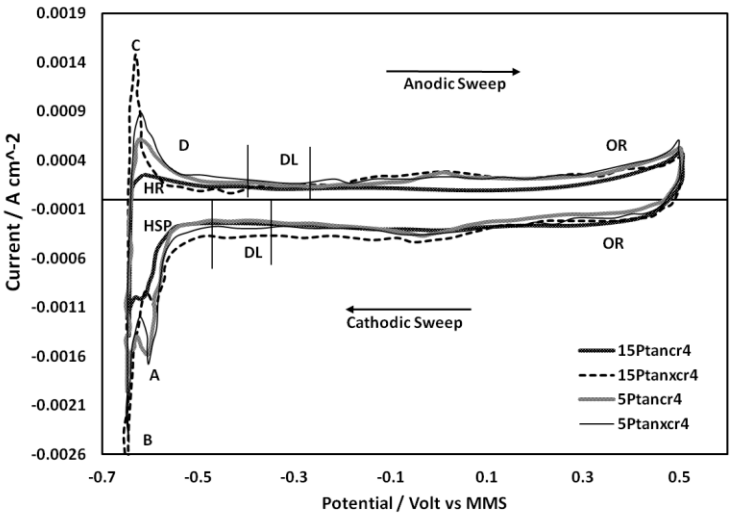

Fig. 2. The CV measurement in 1.0 *mol dm*$^{-3}$ H_2SO_4 solution for a potential range of -0.65 *V* to 0.5 *V* vs MMS reference electrode by the electrodes 15Ptanxcr4, 5Ptanxcr4, 15Ptancr4 and 5Ptancr4, respectively.

A dramatic arising of electrochemical activity was not observed by increasing Pt loading up to 5 wt%. The current change at the hydride region for the electrode 15Ptanxcr4 is about 5.1 *mA*, compared to that of 3 *mA* measured for the electrodes 15Ptancr4 and 5Ptancr4 or 5Ptanxcr4. The discrepancy may be due to following two reasons given by the electrode 15Ptanxcr4: (1) the Pt distributions on zeolite may have been increased; and (2) the Pt particle size is relatively small, resulting in an increase of Pt surface area thus promoting Pt active sites [8, 11]. The formation of the Pt-H adduct in zeolite structure can assist to diminish the sintering of Pt particle during calcinations process, due to the increase of the Pt charge density. The hydrogen adsorption and desorption was found to take place on Pt active sites via hydrogen 'spillover' pathway using carbon made Pt electrode [31], where Pt not in direct contact with Nafion$^{@}$ membrane has been involved in an interfacial process through surface conductance and surface diffusion process [20]. The H^+ ions were able to form an OH group with carbon acidic surface oxides. The electrochemical conductivity in the Pt/Y zeolite carbon powder mixed | Nafion$^{@}$ electrode system might adopt a similar process of either the surface mobility of adsorbed species or the hydrogen adatoms/H^+ ions 'spillover' through the electrode surface via ionic conduction of solution [3, 20]. Zeolite can act as an electron bank to donate or receive electrons, resulting in a 'flow' of protons along acidic sites [32] for H^+ ions being transmitted between Pt active sites on zeolite.

The water was also found to have played a significant role in electrochemical reaction to migrate hydrogen between Pt on zeolite framework by creating zeolite proton conducting membrane strengthening electrode surface conductivity [3, 33]. The electrochemical reaction might involve a charge/electron transfer at the electrode and solution interface in the presence of H^+ and H_3O free species, where ions are transferred by hitching a ride on water during their migration through zeolite channels [3].

3.3. In-situ EXAFS study for 1.5 wt% and 5 wt% Pt/Y zeolite electrocatalysts

The in-situ EXAFS data was collected at the Pt L_{III} edge at room temperature under a potential deposition of -0.65 *V* vs MMS reference electrode in 1.0 *mol* dm^{-3} H_2SO_4 solution. The data was then fitted in R-space by k^3 weighting and the EXAFS spectra were dominated by high Z-value neighbours with phase correction using a computer code EXCURV 98 developed at Daresbury Laboratory, UK.

3.3.1. Pt particle analysis for Pt/Y zeolite electrocatalyst without excess H^+ incorporated in zeolite structure

Figure 3a illustrates the data fitting of the raw EXAFS Chi spectrum ($k^3\chi(k)$ vs *k/Å*) for electrode 15Ptancr4 and their fitted results being presented in table 2. Some data scatterings were observed in Chi spectrum at a slightly high noise level [30]. EXAFS data was subsequently fitted up to 3 shells with a data fitting quality parameter called goodness fitting value (R_{exfd}) of 58% approximately. The curve fitting (in dotted symbols) matches well against the raw data (in solid lines), with shells 1 and 2 Pt-Pt coordination numbers predicted at 7.45 and 2.0, respectively. The data fitting quality was improved by adding a Pt-O shell. This might be attributed by Pt in direct contact with the zeolite support oxygen. The Pt-Pt binding distance is determined at 2.77 *Å*, longer than a standard Pt-Pt binding distance of 2.75 *Å*. This might be introduced by the re-oxidation of OH^- ions on the Pt active sites, where the energy level is coherent to that required for the re-oxidation of OH^- ions.

Figure 3b depicts the EXAFS spectra fitted for electrode 5Ptancr4. Up to four Pt shells were predicted with Pt coordination numbers of 6.78 at shell 1, 1.29 at shell 2, 3.10 at shell 3 and 6.3 at shell 4, respectively. The Pt-Pt binding distance is fitted at 2.76 *Å*. The increase of a Pt bond distance by 0.1 *Å* is possibly due to the H adsorption on the Pt surface and hydrogen evaluation. It might also be associated with the interference of the negative charged zeolite support oxygen atom and Pt particles. No Pt neighbouring oxygen atom was detected; implying Pt particle is fully reduced at -0.65 *V*. The Pt particle size is estimated larger for 5 wt% Pt loading sample than those of 1.5 wt% Pt loading electrocatalysts predicted by Benfield theory [34] using icosahedrons or cubo-octahedron model.

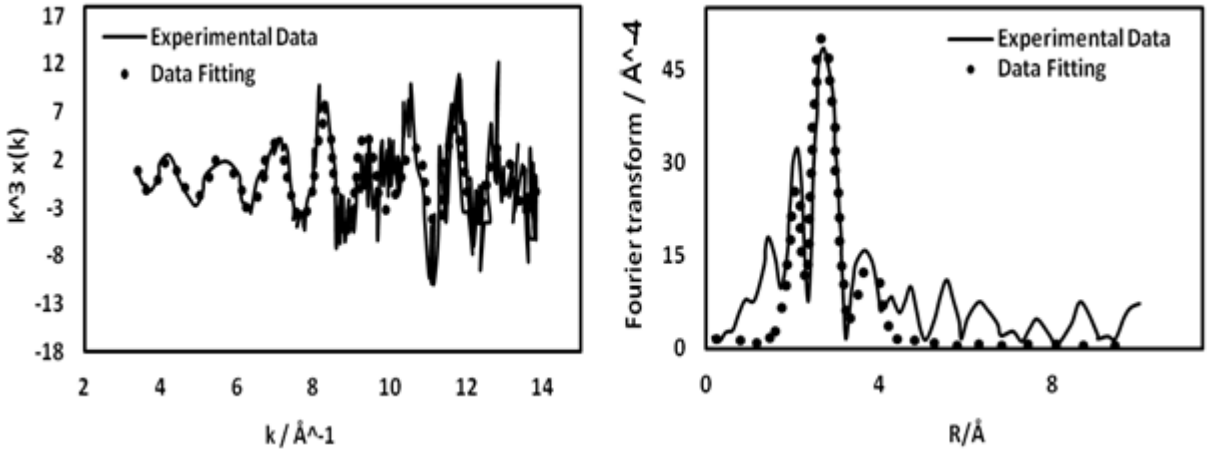

(a) 15Ptancr4

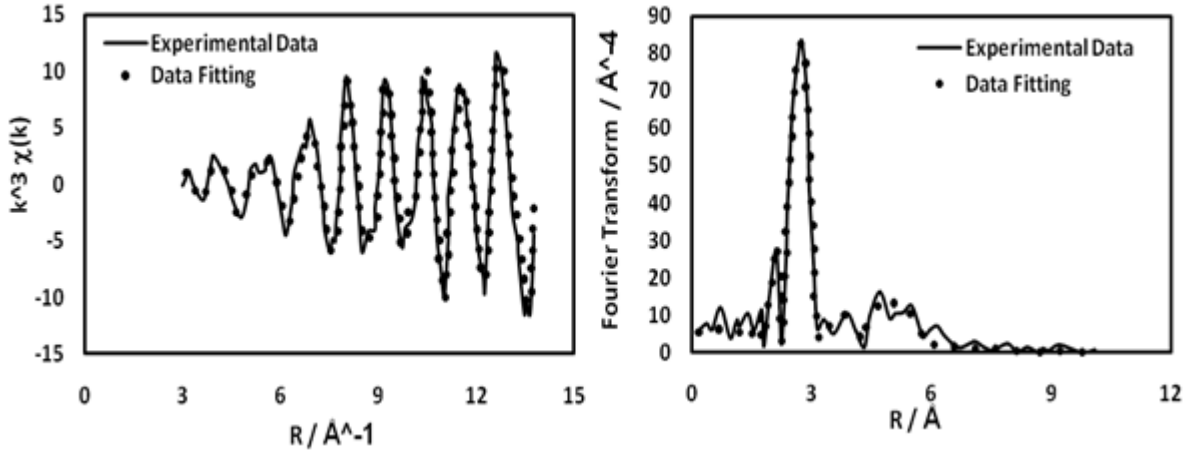

(b) 5Ptancr4

Fig. 3. EXAFS data fitted at the Pt L_{III} edge with phase correction. The experimental data and their fitting results are presented in solid lines and dotted symbols, respectively. Data were collected under a potential disposition at -0.65 *V* vs MMS reference electrode in 1.0 *mol* dm^{-3} H_2SO_4 solution. Samples: (a) 15Ptancr4; (b) 5Ptancr4, both without excess H^+ ions.

3.3.2. Pt particle analysis for Pt/Y zeolite electrocatalyst with excess H^+ ions incorporated in zeolite structure

Figure 4 shows EXAFS spectra fitting for electrocatalysts 15Ptanxcr4 and 5Ptanxcr4 decorated with excess H^+ ions on Y zeolite. A high noise level was shown in raw data of Chi spectrum by sample 15Ptanxcr4, resulted in a slightly poor data quality [30]. The fitting results have been improved by adding the Pt-Pt third shell. This can be confirmed by the reduction of R_{exafs} value to 44.99% approximately. The Pt-Pt first shell coordination number is fitted at 6.38, and that of shells 2 & 3 are predicted at 1.48 and 5.15, respectively. The Pt-Pt binding distance is predicted at 2.77 *Å*, greater than 2.75 *Å* of sample 5Ptanxcr4, possibly attributed by the adsorption of hydrogen (H) on Pt surface or hydrogen evolution. No Pt-O shell was determined around Pt centre atom.

The goodness fitting value of R_{exafs} for sample 5Ptanxcr4 was predicted at 32.24%, approximately. Up to the fourth Pt-Pt shell was fitted with shell 1 Pt-Pt coordination number of 6.78, shell 2 at 1.29, shell 3 at 3.10 and shell 4 at 6.3, respectively. The Pt-Pt binding distance is 2.75 *Å*, indicating that Pt particle is metallic in nature to preserve the bulk Pt property.

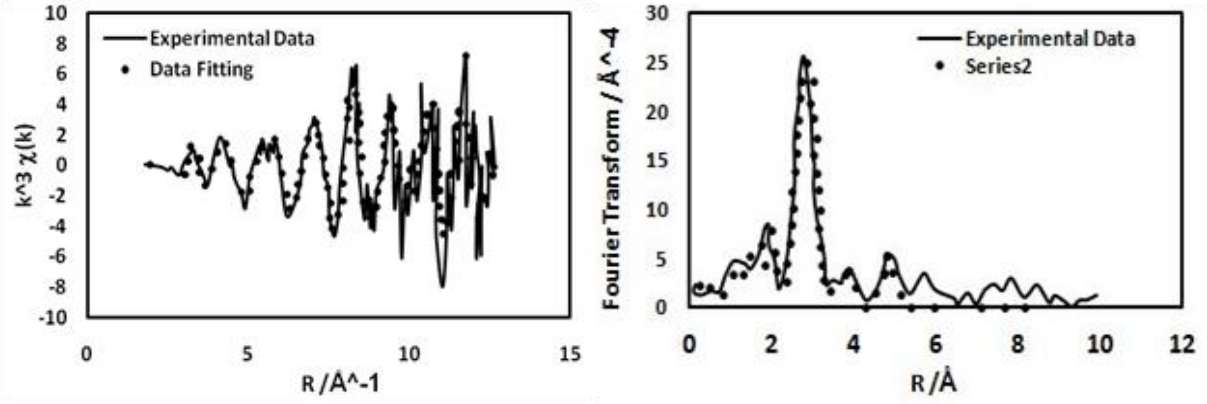

(a) 15Ptanxcr4

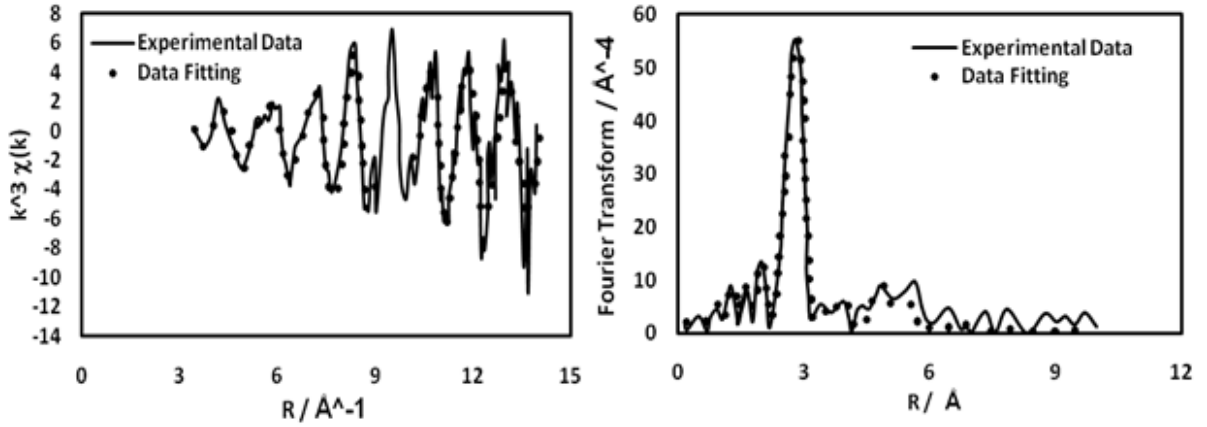

(b) 5Ptanxcr4

Fig. 4. EXAFS data fitted at the Pt L_{III} edge with phase correction. The experimental data and their fitting results are presented in solid lines and dotted symbols, respectively. Data were collected under a potential deposition at -0.65 *V* vs MMS reference electrode in 1.0 *mol* dm^{-3} H_2SO_4 solution. Samples: (a) 15Ptanxcr4; (b) 5Ptanxcr4, both with excess H^+ ions.

Table 2 EXAFS data fitting results for 1.5 wt% and 5 wt% Pt loading Pt/Y zeolite electrocatalyst without excess H^+ ions (i.e. 15Ptancr4, 5Ptancr4) or with excess H^+ ions (i.e. 15Ptanxcr4, 5Ptanxcr4) in presence. The EXAFS data were collected under a potential deposition at -0.65 *V* in 1.0 *mol* dm^{-3} H_2SO_4 solution at room temperature, respectively.

Samples		Shell 1 – O	Shell 2 – Pt	Shell 3 – Pt	Shell 4 – Pt	Shell 5 – Pt
15Ptancr4	N	0.75	7.45	2.05		
	R(*Å*)	2.19	2.77	3.85		
5Ptancr4	N		6.78	1.29	3.10	6.30
	R(*Å*)		2.76	3.89	4.78	5.43
15Ptanxcr4	N		6.38	1.48	5.15	
	R(*Å*)		2.77	3.90	4.80	
5Ptanxcr4	N		5.71	1.50	4.07	5.40
	R(*Å*)		2.75	3.87	4.77	5.40

3.3.3. The ex-situ EXAFS measurement

Although no additional Pt-Pt third shell is predicted for the electrode 15Ptancr4 by in-situ EXAFS measurement, this does not indicate that an average size of Pt is small owing to the presence of O neighbouring atom around the centre of Pt. This has been confirmed by the deterioration of the goodness fitting value of R_{exafs} at 58.87%, compared to that of 44.99% (R_{exafs}) determined for the electrode 15Ptanxcr4. Subsequently, the ex-situ EXAFS analysis was carried out for a further investigation of Pt particle sizes and their distributions on zeolite.

Table 3 presents the fitting results of EXAFS data measured in H_2 gas cell using a mixture of 1.5 wt% or 5 wt% Pt/Y zeolite and boron nitride powder placed between two pieces of plastic film. There is no 'O' atom being predicted for 1.5 wt% Pt sample, indicating Pt might be fully reduced by H_2 gas. A Pt-Pt binding distance was measured to be 2.75 *Å*. The Pt fitting results for sample 15Ptancr4 are in good agreement with that given by Tzou et al. [35]. An average of Pt particle size consists of 17 Pt atoms, significantly higher than the value determined by in-situ measurement.

The number of Pt atoms determined by sample 15Ptanxcr4 in H_2 gas cell consists of 13 atoms in a Pt particle, less than that in sample 15Ptancr4 under electrochemical reaction. This is possibly associated with the reduction of Pt thermal disorder in zeolite system with the increase of Pt binding energy by forming Pt metal proton adduct on zeolite acidic sites during the precursor thermal treatment process [36].

For 5 wt% Pt loading samples (i.e. 5Ptancr4 and 5Ptanxcr4) in H_2 gas phase, the Pt particle size is predicted slightly higher than those determined in electrolyte solution. The data fitting has shown an oxidation of sample 5Ptanxcr4 with O atom detected around the centre of Pt atoms. The Pt-O binding distance is significantly shortened from 2.2 *Å* to 1.93 *Å*, indicating the increase of an average Pt d-orbital binding energy with the increase of charge density on the zeolite support oxygen brought by charge compensation cations of H^+ ions [14]. The Pt-Pt binding distance is determined at 2.75 *Å*, again reflecting the metallic nature of Pt cluster.

Conclusively, a high level of Pt distributions on zeolite is acquired by samples, i.e. 15Ptanxct4 and 5Ptanxcr4 with excess H^+ ions presence. This has been demonstrated by hydrogen adsorption and desorption in hydride region.

Table 3 Data fitting results for 1.5 wt% and 5 wt% Pt/zeolite samples in H_2 gas at room temperature.

Samples		Shell 1 – O	Shell 1 – Pt	Shell 2 – Pt	Shell 3 – Pt	Shell 4 – Pt
15Ptancr4	N		6.33	0.88	3.34	6.40
	R(*Å*)		2.75	3.91	4.78	5.42
5Ptancr4	N		7.47	0.47	4.53	6.57
	R(*Å*)		2.75	3.88	4.79	5.45
15Ptanxcr4	N		6.00	1.59		
	R(*Å*)		2.75	3.90		
5Ptanxcr4	N	0.56	6.02	1.81	4.33	5.93
	R(*Å*)	1.93	2.75	3.89	4.78	5.42

3.4. Electrochemical oxidation of small organic species

The oxidation behaviour of Pt/Y zeolite catalysts was determined by examining the electrooxidation of small organic species, i.e. CH_3OH and HCOOH, as Pt is considered to be the most suitable catalyst for electrooxidation of these small organic molecules [22, 37]. The accompanied by-product of carbon monoxide (CO) to poison Pt surface is examined by CV measurement in a mixture solution of 2.5 $mol\ dm^{-3}$ sulphuric acid (H_2SO_4) and 1 $mol\ dm^{-3}$ of CH_3OH or HCOOH acid. The potential was cycled between -0.65 *V* and 0.5 *V* at a scan rate of 1 $mV\ s^{-1}$, until a clear and stable CV being obtained. The tendency of CV measurement for CH_3OH or HCOOH oxidation is generally in good agreement with that described in literatures [38-40].

Figure 5 displays the CV curves of HCOOH and CH_3OH oxidation on 1.5 wt% and 5 wt% Pt loading zeolite electrocatalysts, presenting a typical current change profile characteristics, which are found consistent to those provided by a commercial Pt/C electrocatalyst (i.e. Johnson Matthey) with a

particle size of 2.5 nm [38]. The HCOOH oxidation starts at a much negative potential region immediately after hydrogen desorption (see, e.g. figure 5a), compared to that determined in CH_3OH (see, e.g. figure 5b), indicating Pt surface is more favourable for HCOOH oxidation than that of CH_3OH. In general, the electrode made by sample 5Ptanxcr4 has shown a better performance to oxidise HCOOH and CH_3OH species. This was evidenced by a dramatic increase of oxidation/reduction current in both the cathodic and anodic sweeps, indicating that most of Pt active surface areas are free from CO occupation and thus available for electrochemical re-oxidation of HCOOH or CH_3OH [38, 39]. A more consistent CH_3OH oxidation/reduction current change was predicted by the electrodes of 15Ptancr4 or 15Ptanxcr4 and 5Ptancr4, respectively, whilst a small discrepancy of current change was determined by an oxidation of HCOOH. Their electrochemical activity follows a decreasing order of 5Ptanxcr4>5Ptancr4 > 15Ptanxcr4 > 15Ptancr5, respectively. The high electrocatalytic activity given by sample 5Ptanxcr4 may be associated with Pt oxidation (Pt-O) state on zeolite due to the interference of Pt with zeolite neighbouring active site, such as Brønsted site (see, e.g. descriptions in sections 3.3.2 and 3.3.3). Present study has shown the increase of Pt loading, i.e. from 1 wt% to 5 wt%, can promote the oxidation of HCOOH or CH_3OH, as seen in high current change, compared to that determined by a commercial Pt/C electrocatalyst at same scan rate of 1 $mV\ s^{-1}$ [38]. Kaur et al. [23] also observed a similar trend using Ce decorated ZSM-5 zeolite as support. This may be due to the attribution given by the interference of metal nanocrystal oxide and zeolite Brønsted acidity of high surface area zeolite, resulting in high stability of catalyst and high electrocatalytic activity [23]. The oxidation mechanism of HCOOH and CH_3OH on Pt electrodes was investigated by various research groups [23, 38-40] with similar conclusions**.** The final by-products given by electrochemical reaction were CO_2 and H_2O, accompanied by intermediate species of HCO and CO. The overall reactions for formic acid and methanol are presented below, respectively:

$$HCOOH + H_2O \longrightarrow 3H^+ + CO_2 + OH^- + 4e^- \quad (9)$$

$$CH_3OH + H_2O \longrightarrow 6H^+ + CO_2 + 6e^- \quad (10)$$

CO was found to be the main poison species involved in the oxidation of methanol and formic acid, resulting in the slowdown of the electrochemical reaction [38-41]. This has been reflected by inhibition of hydrogen adsorption/desorption region. In general, the formation of CO_2 by formic acid (HCOOH) oxidation is much more efficient than that determined for methanol (CH3OH) [39, 42, 43], as evidenced by a high current yield between -0.3 *V* and 0.5 *V* (see, e.g. figure 5a). The present study indicates that both surface oxides and the available solution phase of OH^- ions could be the source of oxygen for the oxidation of CO, in agreement with those published findings [39, 44]. The overall fuel cell efficiency can be subsequently improved in formic acid, where the fuel crossover is much lower than that in methanol, owing to the repulsive interaction among the membrane sulfonic groups and anions [39]. The oxidation of small organic species appears to be a surface process, involving in Pt surface conducting and H^+ ion diffusion and spillover along Pt on zeolite. This is particularly appealing to eletcro-oxidation process of methanol, where a more visible H^+ evaluation/re-oxidation peak was captured by electrode 15Ptanxcr4. The CO oxidation/reduction current due to the disassociation of CH_3OH is generally lower than that predicted by HCOOH, attributed by higher energy density of methanol than that of formic acid. Nevertheless, the low theoretical open circuit potential of methanol can lead to poison Pt surface much easier than that presented in formic acid [38, 44].

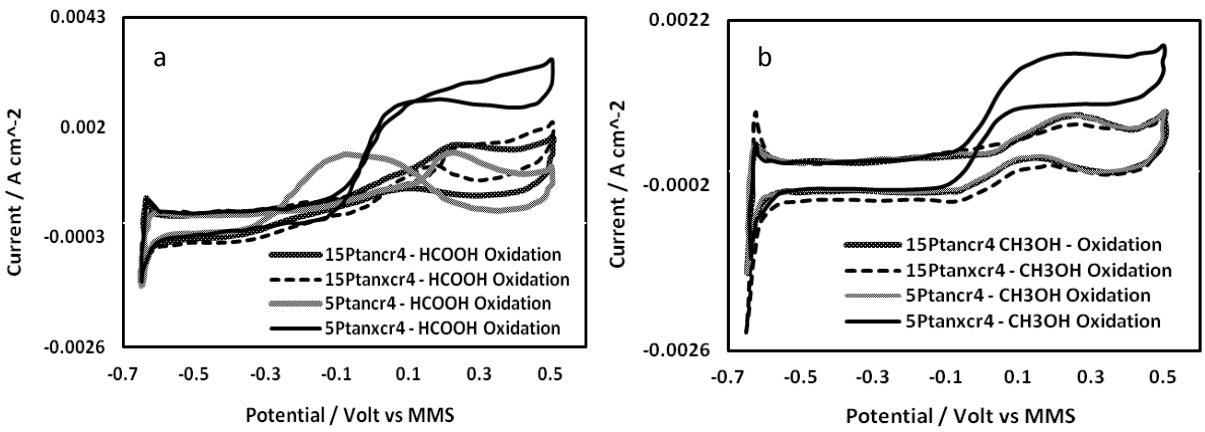

Fig. 5. The steady-state cyclic voltammetry of electrochemical oxidation of HCOOH and CH_3OH on Pt/Y Zeolite catalysts in a mixture solution of 2.5 *mol dm*$^{-3}$ sulphuric acid (H_2SO_4) and 1 *mol dm*$^{-3}$ of HCOOH or CH3OH, respectively. CV measurement was taken until a clear stable CV curve obtained. (a) HCOOH oxidation; (b) CH_3OH oxidation.

4. Pt distribution on Y zeolite

4.1. Estimation of Pt particle size and Pt distribution

The Pt particle size and its geometry were estimated by using the mean value of the first nearest neighbouring coordination number of Pt atoms as a function of Pt cluster edge length [34].

The ex-situ EXAFS measurement data was adopted to estimate the Pt particle, as seen in tables 2 and 3. This is mainly attributed by the following reasons: (1) the low goodness fitting value determined by the ex-situ data fitting, compared to those using in-situ EXAFS data; (2) Pt particles were fully reduced on zeolite in H_2 gas, along with well-preserved zeolite structure (i.e. BET surface area at 539 m^2g^{-1} or for 563 m^2g^{-1} for 15anxcr4 or 5anxcr4, respectively); and (3) Pt particles might not follow icosahedral model under a potential deposition for in-situ measurement. The diameter of average Pt particle size is likely to increase in an acidic solution [46], particularly under potential deposition in hydride region. Table 4 illustrates the number of Pt atoms and their distributions in a Pt cluster. The Pt particle size is estimated around 1.0 - 1.1 nm in diameter with 147 atoms in a Pt cluster for sample 15Ptancr4 without excess H^+ ions on zeolite and 5 wt% Pt loading samples (i.e. 5Ptanxcr4 and 5Ptancr4). However, a significant decrease of Pt particle size down to about 0.55 - 0.82 nm is determined for sample 15Ptanxcr4 in the presence of excess H^+ ions in zeolite structure, consisting of merely 13 to 55 atoms in a Pt cluster. The presence of H^+ ions on zeolite surface may facilitate the change of the charge density of zeolite support oxygen, resulting in a large reduction of Pt particle size.

Table 4 The average first nearest neighbouring coordination number of Pt atoms and the number of Pt atoms in a Pt cluster.

Acronym name	15Ptancr4	15Ptanxcr4	5Ptancr4	5Ptanxcr4[a]
$\overline{N_l}$ from refinement - Pt	6.33	6.00	7.47	6.02
Total atom in a Pt cluster	147	13, 55	147	147
Particle size (nm)	1.0 - 1.1	0.55 - 0.82	1.0 - 1.1	1.0 - 1.1

[a]Oxygen neighbours present in the first Pt–O coordination shell.

4.2. Pt active surface area and distribution on zeolite

The actual Pt loading was calculated using an edge jump from EXAFS subtraction [29]. The surface area of Pt particle was determined via hydrogen adsorption and desorption peaks captured by cyclic voltammetry measurement in H_2SO_4 solution. Table 5 illustrates a comparison of Pt distributions on zeolite for 1.5 wt% and 5 wt% Pt loading samples.

A significant high Pt surface area was determined for sample 15Ptanxcr4. The actual Pt loadings on zeolite for samples 15Ptanxcr4 and 15Ptancr4 are 0.77 wt% and 1.52 wt% respectively, in consistent to Pt active surface areas of 103.57 m^2g^{-1} and 51.59 m^2g^{-1}. The Pt surface area is found generally low for the samples of 5Ptanxcr4 and 5Ptancr4, estimated at 32.61 m^2g^{-1} and 21.47 m^2g^{-1}, with correspondent to Pt loadings of 4.71 wt% and 7.76 wt%, respectively. The prepared Pt loading on zeolite for samples 15Ptancr4 and 5Ptanxcr4 is found consistent with the measured values for 1.5 wt% and 5 wt% Pt loading on Y zeolite, whilst either a significant low or a significant high value is determined for samples 15Ptanxcr4 and 5Ptancr4, respectively.

The net Pt atoms per cm^2 (N_T) predicted for samples 5Ptancr4, 5Ptanxcr4, 15Ptancr4 and 15Ptanxcr4 were followed an order of $26.42 \times 10^{17} > 16.16 \times 10^{17} > 5.21 \times 10^{17} > 2.64 \times 10^{17}$ per cm^2, respectively. This tendency of net Pt atom distribution per cm^2 is well reflected by Pt loading on Y zeolite. The associated Pt surface atoms per cm^2 on zeolite (N_S) were determined to be 13.11×10^{16} (for sample 5Ptancr4) > 15.11×10^{16} (for sample 5Ptanxcr4) > 7.64×10^{16} (for sample 15Ptancr4) > 7.77×10^{16} (for sample 15Ptanxcr4), respectively. This has provided a high level of Pt surface atom dispersions (defined as $N_S/N_T \times 100\%$) of 29.44% for sample 15Ptanxcr4, compared with the values of 14.66%, 9.35% and 4.93% for samples 15Ptancr4, 5Ptanxcr4 and 5Ptancr4, respectively. In general, the excess H^+ ions incorporated with Pt/Y zeolite electrocatalyst will result in a better Pt surface atom dispersion, compared to samples with Pt loading at same level without excessive H^+ ion presence. The increase of Pt loading on zeolite from 1.5 wt% to 5 wt% loading does not provide a higher Pt surface dispersion.

The present study has shown that H^+ ions enable to achieve high Pt distribution on zeolite, owing to the change of Pt d bond energy state. The high Pt surface area can contribute to improve the Pt electrocatalytic activity using Nafion@ bound Pt electrode, i.e. 15Ptanxcr4 or 5Ptanxcr4. This has been clearly reflected by the electrochemical reactions on Pt surface as (1) hydrogen

oxidation/reduction in hydride region in 2.5 *mol dm*$^{-3}$ H_2SO_4 solutions, and (2) the oxidation of small organic species, i.e. HCOOH and CH_3OH species, in a 2.5 *mol dm*$^{-3}$ H_2SO_4 electrolyte solution containing 1 *mol dm*$^{-3}$ HCOOH or CH_3OH species. The increase of Pt loading on zeolite is able to facilitate the oxidation of HCOOH or CH_3OH species, which supports the evidence found by Kaur et al. [23].

For electrocatalysts, i.e. 15Ptanxcr4 and 5Ptanxcr4, H^+ ions act in a very similar way as other ions such as K^+, Ca^{2+} and Fe^{2+} to promote a better Pt particle distribution by anchoring Pt on the zeolite surface and supercage wall to restrain Pt migration. Present CV measurement implies that the Pt particle sizes and their distributions on zeolite are indeed one of major contributors to determine the Pt oxidation and reduction performance.

Table 5 The comparison of Pt distributions on zeolite for 1.5 wt% and 5 wt% Pt loading samples.

Electrocatalyst	15Ptancr4	15Ptanxcr4	5Ptancr4	5Ptanxcr4[a]
Pt active surface area m^2g^{-1}	51.29	103.57	21.47	32.61
Calculated mass quantity in wt %	1.52	0.77	7.76	4.71
N_T Pt net atoms per cm^2 ($\times 10^{17}$)	5.21	2.64	26.62	16.16
N_S Pt surface atoms per cm^2 ($\times 10^{16}$)	7.64	7.77	13.11	15.11
Dispersion N_S/N_T (%)	14.66	29.44	4.93	9.35

Note: N_T is Pt total atoms per cm^2; and N_S is obtained from Benfield theory.

5. Conclusion

This paper has presented the characteristics of zeolite supported Pt nano-particle and their electrocatalytic performances by EXAFS analysis and CV measurements. The resultant data analysis indicates that H^+ ions were able to restrain the mobility of Pt on zeolite during precursor thermal treatments by anchoring Pt on zeolite cage wall, leading to a high dispersion of Pt on zeolite and a better electrocatalytic performance, i.e. 15Ptanxcr4 and 5Ptanxcr4, compared to samples without the excess H^+ on zeolite, i.e. 15Ptancr4 and 5Ptancr4.

The Pt-Pt binding distance was measured between 2.75 *Å* and 2.77 *Å*, indicating the metallic nature of Pt. The 0.1 *Å* or 0.2 *Å* increase of Pt-Pt binding distance over a standard value of 2.75 *Å* could be attributed by either electrochemical adsorption of H atom on Pt active surface forming a Pt-H bond or the interference of zeolite support oxygen as a result of increasing oxygen charge density. This can facilitate the oxidation of CH_3OH and HCOOH species, as evidenced by CV measurement using sample such as 5Ptanxcr4.

The hydrogen spillover pathway was explored by depicting the charger/electron transfer at Pt electrode and solution interface by either the direct charger transfer or the mobility of H_{ads}/H^+ species on zeolite, which is a DC electrical insulator. The H^+ ions were found able to transmit along the zeolite surface to increase the surface conductivity of catalyst. The H^+ and H_3O^+ ions may also

lead to ionic conduction via free species by hitching a ride on water to increase the electrode surface conductivity. In general, HCOOH has shown a better oxidation performance than that of CH_3OH.

References

[1] Min MK, Cho J, Cho K, Kim H. Particle size and alloying effects of Pt based alloy catalysts for fuel cell applications. Electrochimica Acta 2000; 45: 4211–4217.

[2] Han W, Kwan SM, Yeung LK. Zeolite application in fuel cell: water management and proton conductivity. Chemical Engineering Journal 2012; 187: 367-371.

[3] Breck DW. Zeolite molecular sieves: structure, chemistry and use. New York: Wiley – Interscience; 1974.

[4] Rolison DR. Zeolite-modified electrodes and electrode-modified zeolites. Chemical Reviews 1990; 90: 867-878.

[5] Sachtler WMH, Zhang ZC. Zeolite-supported transition metal catalysts. Advances in Catalysis 1993; 39: 129-220.

[6] Exner D, Jaeger N, Kleine A, Schulz-Ekloff G. Reduction–agglomeration model for metal dispersion in platinum-exchanged NaX zeolite. J. Chem. Soc. Faraday Trans.1: Physical Chemistry in Condensed Phase 1988; 84: 4097-4104.

[7] Reagan WJ, Chester AW, Kerr GT. Studies of the thermal decomposition and catalytic properties of some platinum and palladium ammine zeolites. J. of Catalysis 1981; 69(1): 89-100.

[8] Gallezot P, Alarcon-Diaz A, Dalmon JA, Renouprez AJ, Imeuk B. Location and dispersion of platinum in Pt/Y zeolites. J. of Catalysis 1975; 39: 334 - 349.

[9] Tzou MS, Teo BK, Sachtler WMH. Formation of Pt particles in Y-type zeolites: the influence of coexchanged metal cations. J. of Catalysis 1998; 113: 220-235.

[10] Tao L, Dou S, Ma ZL, Shen AL, Wang SY. Simultaneous Pt deposition and nitrogen doping of graphene as efficient and durable electrocatalysts for methanol oxidation. International of Journal Hydrogen Energy 2015; 40: 14371-14377.

[11] Bergeret G, Gallezot P, Imelik B. X-ray study of the activation, reduction, and re-oxidation of palladium in Y-type zeolites. J. Phys. Chem. 1981; 85(4): 411-416.

[12] Koningsberger DC, de Graaf J, Mojet BL, Ramaker DE, Miller JT. The metal–support interaction in Pt/Y zeolite: evidence for a shift in energy of metal d-valence orbitals by Pt–H shape resonance and atomic XAFS spectroscopy. Applied Catalysis A: General 2000; 191: 205 -220.

[13] Mojet BL, Miller JT, Ramaker DE, Koningsberger DC. A new model describing the metal–support interaction in noble metal catalysts. J. of Catalysis 1999; 186: 373-386.

[14] Zhang ZC, Wong TT, Sachtler WMH. The effect of Ca^{2+} and Mg^{2+} ions on the formation of electron-deficient palladium-proton adducts in zeolite Y. J. of Catalysis 1991; 128: 13-22.
[15] Larsen G, Haller GL. Metal-support effects in Pt/L-zeolite catalysts. Catalysis Lett. 1989; 3: 103-110.
[16] Pandya KI, Heald SM, Hriljac JA, Petrakis L, Fraissard J. Characterization by EXAFS, NMR, and other techniques of Pt/NaY zeolite at industrially relevant low concentration of platinum. Journal of Physical Chemistry 1996; 100(12): 5070-5077.
[17] Boyanov BI, Morriso TI. Support and temperature effects in platinum clusters 1: spatial structure. Journal of Physical Chemistry 1996; 100: 16310-16317.
[18] Yakoyama T, Kosugi N, Asakura K, Iwasawa Y, Kuroda H. Temperature dependence of the Pt L3-edge EXAFS of platinum clusters supported on NaY-zeolite. Journal De Physique 1986; C8: 273-276.
[19] Vaarkamp M, Modica FS, Miller JT, Koningsberger DC. Influence of hydrogen pre-treatment on the structure of the metal-support interface in Pt/zeolite catalysts. J. of Catalysis 1993; 144(2): 611-626.
[20] Liu W-J, Wu B-L, Cha C-S. Surface diffusion and the spillover of H-adatoms and oxygen–containing surface species on the surface of carbon black and Pt/C porous electrodes. J. Electro-analytical Chem. 1999; 476(2): 101-108.
[21] Zhang A, Nakamura I, Fujimoto K. A new probe reaction for studying the hydrogen spillover phenomenon. Journal of Catalysis 1997; 168(2): 328-333.
[22] Hernandez-Fernandez P, Lund PB, Kallesøe C, Clausen HF, Christensen LH. Supported Pt-based nanoparticulate catalysts for the electro-oxidation of methanol: an experimental protocol for quantifying its activity. International Journal of Hydrogen Energy 2015; 40: 284-291.
[23] Kaur B, Srivastava R, Satpati B. Highly efficient CeO_2 decorated nano-ZSM-5 Catalyst for electrochemical oxidation of methanol. American Chemical Society (ACS) Catal. 2016; 6: 2654-2663.
[24] Hsieh CT, Chen WY, Tzou DY, Roy AK, Hsiao HT. Atomic layer deposition of Pt nanocatalysts on graphene oxide nanosheets for electro-oxidation of formic acid. International Journal of Hydrogen Energy 2012; 37: 17873-17843.
[25] El-Nagar GA, Mohammed AM. Enhanced electrocatalytic activity and stability of platinum, gold, and nockel oxide nanoparticles based ternary catalyst for formic acid electro-oxidation. International Journal of Hydrogen Energy 2014; 39: 11955-11962.
[26] Bessel CA, Rolison DR. Micro-heterogeneous dispersion electrolysis with nano-scale electrode - modified zeolite. Journal of Electro-analytical Chemistry 1997; 439: 97-105.

590 [27] Persaud L, Bard AJ, Campion A, Fox MA, Mallouk TE, Webber SE, White JM. A new method for
591 depositing platinum exclusively on the internal surface of zeolite L. Inorg. Chem. 1987; 26: 3825 -
592 3827.
593 [28] Brett CMA, Brett AMO. Electroanalysis. Oxford University Press, 1998.
594 [29] Abruna HD. X-ray absorption spectroscopy in the study of electrochemical system. In: HD
595 Abruna (Eds.), Electrochemical interface: modern techniques for in-Situ interface characterization.
596 New York: VCH Publishers; 1991, Chapter 1: pp.1-54
597 [30] Yao J, Yao YF. Proton modified Pt zeolite fuel cell electrocatalysts. In: Sayigh A (Eds.),
598 Renewable energy in the service of mankind, Vol 1, selected topic from world renewable energy
599 congress WPEC 2014. Springer International Publishing, Switzerland, 2015, pp. 173 -182.
600 [31] Srinivas S, Rao P. Direct observation of hydrogen spillover on carbon-supported platinum and its
601 influence on the hydrogenation of benzene. J. of Catalysis 1994; 148(2): 470-477.
602 [32] Ueda P, Kusakari T, Tomishige K, Fujimoto K. Nature of spiltover hydrogen on acid sites in
603 zeolite: observation of the behaviour of adsorbed pyridine on zeolite catalysts by means of FTIR. J. of
604 Catalysis 2000; 194(1): 14-22.
605 [33] Herrmann JM, Pichat P. Evidence by electrical conductivity measurements for hydrogen
606 spillover on Pt, Rh and Ni/TiO_2 catalysts: consequences for bufunctional photocatalysis. In: Pajonk
607 GM, Teichner SJ, Germain JE, editors. Spillover of Adsorbed Species, Studies in Surface Science and
608 Catalysis. Elsevier, Amsterdam, 1983, pp. 77-88.
609 [34] Benfield RE. Mean coordination numbers and the non-metal-metal transition in cluster. J. of the
610 Chem. Soc. Faraday Trans. 1992; 88(8): 1107-1110.
611 [35] Tzou MS, Kusunoki M, Asakura K, Kuroda H, Moretti G, Sachtler WMH. Bimetallic copper-
612 platinum particle supported in Y zeolite: structural characterization by EXAFS. J. Phys. Chem. 1991;
613 95(13): 5210-5215.
614 [36] Rolison DR, Hayes EA, Rudzinski WE. Electrode-modified zeolites: electrode microstructures
615 contained in and on a heterogeneous catalyst. J. of Phys. Chem. 1989; 93(14): 5524-5531.
616 [37] Frelink T, Visscher W, Cox AP, van Veen JAR, Bunsenges B. The role of surface oxides in the
617 electrooxidation of methanol, formic acid and CO on Pt, Ru and codeposited Pt-Ru. Phy. Chem. 1996;
618 100: 599-606.
619 [38] Wang ZB, Chu YY, Shao AF, Zuo PJ,, Yin GP, Electrochemical impedance studies of
620 electrooxidation of methanol and formic acid on Pt/C catalysts in acid medium, Journal of Power
621 Sources 2009; 190: 336-340.

622 [39] Lovic JD, Tripkovic AV, Gojkovic SL J, Popovic K, Tripkovic DV, Olszewski P, Kowal A. Kinetic study
623 of formic acid oxidation on carbon supported platinum electrocatalyst. J. Electroanal. Chem. 2005;
624 581: 294 – 302.
625 [40] Zhao L, Wang ZB, Li JL, Zhang JJ, Sui XL, Zhang LM. Hybrid of carbon-supported Pt nanoparticles
626 and three dimensional graphene aerogel as high stable electrocatalysts for methanol
627 electrooxidation. Electrochimica Acta 2016, 189: 175-183.
628 [41] Cai GX, Guo JW, Wang J, Li S. Negative resistance for methanol electro-oxidation on
629 platinum/carbon (Pt/C) catalyst investigated by an electrochemical impedance spectroscopy. J of
630 Power Sources 2015; 276: 279-290.
631 [42] Markovic NM, Gasteiger HA, Ross PN, Jiang XD, Villegas I, Weaver M. Electro-oxidation
632 mechanisms of methanol and formic acid on Pt-Ru alloy surfaces. Electrochimica Acta 1995; 40(1):
633 91-98.
634 [43]. Herrero E, Franaszczuk K, Wieckowski A. Electrochemistry of methanol at low index crystal
635 planes of platinum: an integrated voltammetric and chronoamperometric study. J. Phys. Chem.
636 1994; 98: 5074-5083.
637 [44] Njagi EC, Genuino HC, King'ondu CK, Chen CH, Horvath D, Suib SL. Preferential oxidation of CO
638 in H2-rich feeds over mesoporous copper manganese oxides synthesized by a redox method.
639 International Journal of Hydrogen Energy 2011; 36: 6768-6779.
640 [45] Kang SJ, Lee JY, Lee JK, Chung SY, Tak YS. Influence of bi modification of Pt anode catalyst in
641 direct formic acid fuel cells. J. Phys. Chem. B 2006; 110: 7270-7274.
642 [46] Ranasinghe AD. Part I: In situ pulse electrochemical deposition of Pt nanoparticles for efficient
643 catalyst utilization in fuel cell. PhD Thesis, University of California Santa Barbara, 2007. Publication
644 Number: AAI3274422; ISBN: 9780549152644; Source: Dissertation Abstracts International, Volume:
645 68-07, Section: B, page: 4441; 199 p.